

Small- x Effects in W + jets Production at the Tevatron

Leif Lönnblad

Theory Division, CERN
CH-1211 Genève 23, Switzerland
E-mail: Leif.Lonnblad@cern.ch

Abstract

The jet structure in events with Drell-Yan-produced W bosons is discussed, and a new model for describing such event is presented. The model is shown to explain recent measurements of the W -jet rapidity correlation and predicts a transverse energy flow at high W rapidities (corresponding to probing small- x partons in one of the incoming protons) higher than conventional parton cascade event generators.

Submitted to Nucl. Phys. B

1 Introduction

The description of small- x partons within hadrons has attracted a great deal of interest, especially after the measurements of the proton structure function F_2 at x values down to 10^{-4} at HERA, where a substantial increase was found [1,2]. Although the small- x rise was first predicted by the so-called BFKL evolution equation [3,4] it soon turned out [5,6] that it could also be explained in terms of the conventional Altarelli–Parisi (DGLAP) evolution equations [7–10]. Instead, much of the focus has been directed towards the study of hadronic final states in deep inelastic lepton–hadron scattering (DIS) events at small x , and it has been suggested that the large flow of transverse energy in the proton direction found in such events is a signal of BFKL dynamics [11].

Much can also be learned from comparing data with different models implemented in Monte Carlo event generators. So far it has been shown that generators built around a conventional DGLAP-inspired initial-state parton showers, such as PYTHIA [12,13] and LEPTO [14], with strong ordering in virtuality, completely fail to describe things like the forward transverse energy flow at small x , while a generator such as ARIADNE [15] – although not implementing BFKL evolution, but sharing with it the feature that emissions are unordered in transverse momenta – describes such event features quite well [16,17].

Besides deep inelastic lepton–hadron scattering, Drell–Yan production in hadron–hadron collisions is one of the cleanest probes of hadronic structure. Recent results from the D0 collaboration [18] at the Tevatron shows a surprising feature of events with Drell–Yan-produced W bosons, namely the decorrelation in rapidity between the W and the associated jets. Although the typical x -values probed in W events at the Tevatron is on the order of $\sqrt{m_W^2/S} \approx 80/1800 \approx 0.04$, for large rapidities of the W , one of the incoming partons has a much smaller momentum fraction of the proton (e.g. $y_W \approx 2$ gives $x_1 \approx 6 \times 10^{-3}$ and $x_2 \approx 0.3$). Therefore it could be worth while to take the experience gained from studying small- x final states at HERA and try to apply it to large rapidity W -production at the Tevatron.

In this paper the Dipole Cascade Model (DCM) [19,20], on which the ARIADNE program is built, is extended to also model the jet structure of Drell–Yan production events. The main feature of the DCM for DIS [21] is that gluon emission is treated as final state radiation from the colour dipole formed between the struck quark and the proton remnant as in fig. 1a. In this way there is no explicit initial state radiation, and the proton structure enters only in the way the dipole radiation is suppressed due to the spatial extension of the proton remnant. This approach has some problems when it comes to describing features particular to the initial state, such as the initial splitting of a gluon into a $q\bar{q}$ -pair.

The simplest extension of the DCM to also treat Drell–Yan production would be to treat gluon emission as final-state radiation from the colour dipole formed between the two remnants, as in fig. 1b. However, as is seen from fig. 2, the leading order W +jet diagrams all

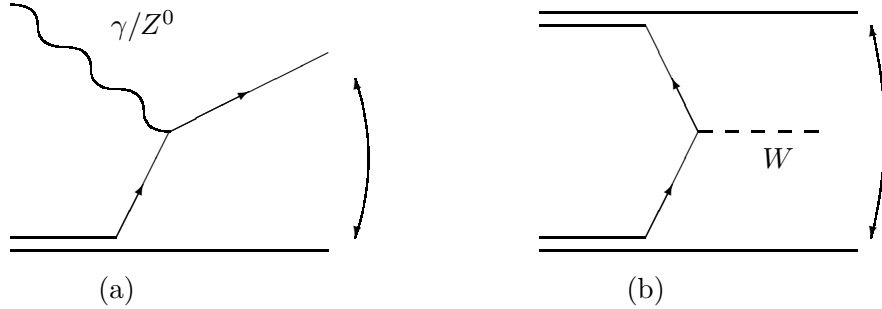


Figure 1: *The colour dipoles that initiate the dipole cascade in (a) DIS and (b) Drell-Yan production of W .*

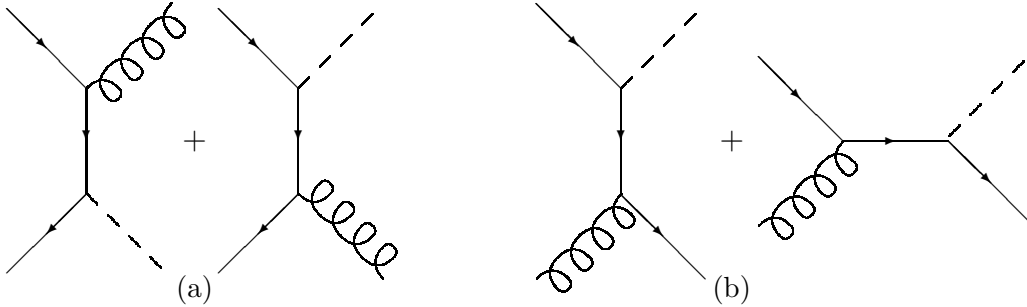


Figure 2: *The leading-order Feynman diagrams contributing to $W + \text{jet}$ production corresponding to the annihilation (a) and Compton (b) diagrams.*

correspond to initial-state radiation (except for the last one, which is the least important). And in particular it is clear that if the gluon emission is treated as final-state radiation between the two remnants, it would be difficult to explain the contribution to the transverse momentum of the W from the diagrams in fig. 2.

In previous work [22] the DCM was extended to also include the boson-gluon fusion diagram in DIS, which can be viewed as a special case of initial-state gluon splitting into $q\bar{q}$. In this paper, this approach is further developed into a general inclusion of initial-state gluon splitting into $q\bar{q}$. Also, a way is presented of taking into account the contribution to the transverse momentum of the W from the gluon emission, formulated it terms of radiation from the colour dipole between the two proton remnants.

The layout of this paper is as follows. In sections 2 and 3 the treatment of gluon emission and initial state gluon splitting is presented. In section 4, results for the W -jet rapidity correlation from the improved DCM is compared to a leading-order calculation and with the conventional DGLAP-inspired initial-state parton shower approach of PYTHIA. Also some predictions are given for the transverse energy flow in high rapidity W events at Tevatron energies. Finally, in section 5, the conclusions are presented.

2 Gluon Emission

The DCM for e^+e^- annihilation and deep inelastic lepton-hadron scattering is described in detail in refs. [19–21] and only a brief summary of the features important for this paper will be given here.

The emission of a gluon g_1 from a $q\bar{q}$ pair created in an e^+e^- annihilation event can be described as radiation from the colour dipole between the q and \bar{q} . A subsequent emission of a softer gluon g_2 can be described as radiation from two independent colour dipoles, one between the q and g_1 and one between g_1 and \bar{q} . Further gluon emissions are given by three independent dipoles etc.

In DIS, the gluon emission comes from the dipole stretched between the quark, struck by the electro-weak probe, and the hadron remnant. The situation is the same as in e^+e^- above, except that, while q and \bar{q} are both point-like in the case of e^+e^- , the hadron remnant in DIS is an extended object. In an antenna of size l , radiation with wavelengths $\lambda \ll l$ are strongly suppressed. In the DCM, this is taken into account by only letting a fraction

$$a = \mu/k_\perp \quad (1)$$

of the hadron remnant take part in the emission of a gluon with transverse momentum k_\perp , where μ is a parameter corresponding to the inverse (transverse) size of the hadron.

The phase space available in dipole emission is conveniently pictured by the inside of a triangle in the κ - y plane, where $\kappa \equiv \ln k_\perp^2$ and y is the rapidity of the emitted gluon as in fig. 3. In these variables the dipole emission cross section also takes a particularly simple approximate form:

$$d\sigma \propto \alpha_S d\kappa dy. \quad (2)$$

In DIS, assuming that the hadron is coming in with momentum (using light-cone coordinates) $(P_+, 0, \vec{0})$, and is probed by a virtual photon $(-Q_+, Q_-, \vec{0})$, the triangular area comes from the trivial requirement

$$\begin{aligned} k_{+g} &\equiv k_\perp e^y < P_+ \\ k_{-g} &\equiv k_\perp e^{-y} < Q_-. \end{aligned} \quad (3)$$

The condition that only a fraction of the remnant participates in an emission means that

$$k_{+g} < (\mu/k_\perp) P_+ \quad (4)$$

and translates into an extra cutoff in the phase space corresponding to the thick line in fig. 3. This should be compared to the initial-state parton shower scenario, where gluon emission is given by

$$d\sigma_q = \frac{2\alpha_S}{3\pi} \frac{1+z^2}{1-z} \frac{f_q(x/z)}{f_q(x)} \frac{dz}{z} \frac{dQ^2}{Q^2}. \quad (5)$$

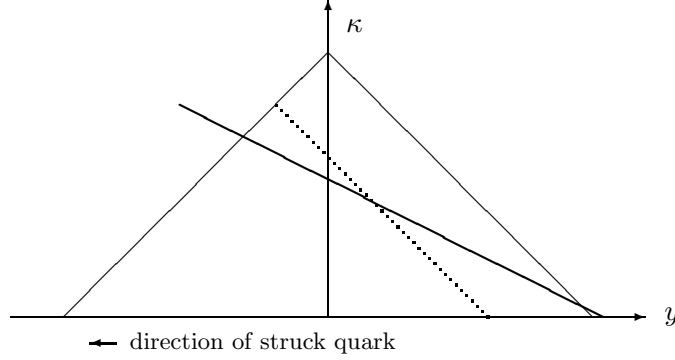


Figure 3: *The phase space available for gluon emission in DIS (thin lines) and the extra restriction due to the extendedness of the proton remnant (thick line). The dotted line corresponds to a line of equal suppression due to the ratio of parton density functions entering into a conventional parton shower scenario.*

Identifying the ratio of structure functions in eq. (5) (corresponding to the dotted line of equal suppression in fig. 3) with the extra cutoff (4) in the DCM, the two models are equivalent in the low- k_{\perp} limit.

As mentioned in the introduction, the simplest way of extending the DCM to describe gluon emissions in Drell–Yan events is to describe it as radiation from the colour dipole between the two hadron remnants. One problem with this approach is what to do with the transverse recoil from the gluon emission. In e^+e^- , this recoil is shared by the q and \bar{q} . In DIS, since only a fraction of the remnant is taking part in the emission, only that fraction is given a transverse recoil, resulting in an extra, so-called recoil gluon [21]. The corresponding procedure for Drell–Yan would be to introduce two recoil gluons, one for each remnant. However in that way it is impossible to reproduce the transverse momentum of the W as given by the $\mathcal{O}(\alpha_S)$ matrix element.

The $\mathcal{O}(\alpha_S)$ matrix element for $q + \bar{q} \rightarrow W + g$ production takes the form [23]

$$M^{q\bar{q} \rightarrow Wg} \propto \frac{\hat{t}^2 + \hat{u}^2 + 2m_W^2 \hat{s}}{\hat{t}\hat{u}}, \quad (6)$$

where \hat{s} , \hat{t} and \hat{u} are the ordinary Mandelstam variables satisfying $\hat{s} + \hat{t} + \hat{u} = m_W^2$. In order to reproduce this in a parton shower scenario, where the gluon is emitted “after” the W is produced, this has to be convoluted with the parton density functions, and the lowest-order W -production matrix element, again convoluted with the relevant parton densities, has to be factored out. This introduces some ambiguities, which are solved by assuming that the rapidity of the W is the same before and after the gluon emission, resulting in the following cross section, expressed in the transverse momentum k_{\perp}^2 and rapidity y_g of the emitted gluon

$$\frac{d\sigma_g}{dy_g dk_{\perp}^2} = \frac{2\alpha_S}{3\pi} \frac{f_q(x'_q) f_{\bar{q}}(x'_q)}{f_q(x_q) f_{\bar{q}}(x_{\bar{q}})} \times$$

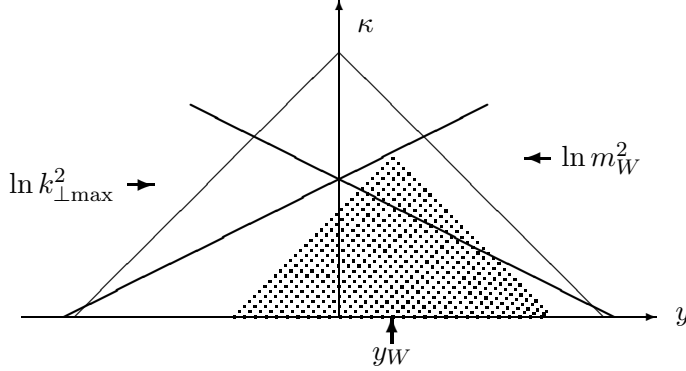


Figure 4: The phase space available for gluon emission in W production (thin lines) and the extra restriction due to the extendedness of the proton remnants (thick lines). The shaded triangle corresponds to the phase space area covered by the W .

$$\frac{(k_{\perp}^2 + m_{\perp}^2 + k_{\perp} m_{\perp} e^{\Delta y})^2 + (k_{\perp}^2 + m_{\perp}^2 + k_{\perp} m_{\perp} e^{-\Delta y})^2}{(k_{\perp}^2 + k_{\perp} m_{\perp} e^{\Delta y})(k_{\perp}^2 + k_{\perp} m_{\perp} e^{-\Delta y})(k_{\perp}^2 + m_{\perp}^2 + k_{\perp} m_{\perp} (e^{\Delta y} + e^{-\Delta y}))}, \quad (7)$$

where $\Delta y = y_g - y_W$, $m_{\perp}^2 = k_{\perp}^2 + m_W^2$, y_W the rapidity of the W and x_i and x'_i the energy-momentum fractions carried by the incoming partons before and after the gluon emission so that

$$x_q = \frac{m_W e^{y_W}}{\sqrt{S}}, \quad x'_q = \frac{m_{\perp} e^{y_W} + k_{\perp} e^{y_g}}{\sqrt{S}}, \quad (8)$$

$$x_{\bar{q}} = \frac{m_W e^{-y_W}}{\sqrt{S}}, \quad x'_{\bar{q}} = \frac{m_{\perp} e^{-y_W} + k_{\perp} e^{-y_g}}{\sqrt{S}}, \quad (9)$$

assuming the q coming in along the positive z -axis and a total invariant mass of \sqrt{S} .

In the limit $k_{\perp}^2 \ll m_W^2$, eq. (7) reduces to the simple dipole emission cross section in eq. (2), so it is clear that the strategy outlined above is a good leading log approximation. It also turns out that it is fairly simple to correct the first gluon emission so that, disregarding the ratios of parton densities, eq. (7) is reproduced.

The ratio of parton densities in eq. (7) is instead approximated by the suppression of the phase space introduced for DIS in eq. (4), which in this case corresponds to suppressions on both sides of the triangle, as in fig. 4. One problem with this procedure is that the k_{\perp}^2 of the gluon and hence of the W is limited by this suppression to

$$k_{\perp}^2 < \mu \sqrt{S/4}, \quad (10)$$

which, with $\mu \approx 1$ GeV, gives $k_{\perp} \lesssim 30$ GeV. To be able to describe high- k_{\perp} W production, it is clear that the sharp cutoff in fig. 4, which in any case is an oversimplification, must be replaced by a smooth suppression. In [21] it was shown that introducing a power suppression in the disallowed regions in fig. 3 does not influence the general event shapes in DIS; it is

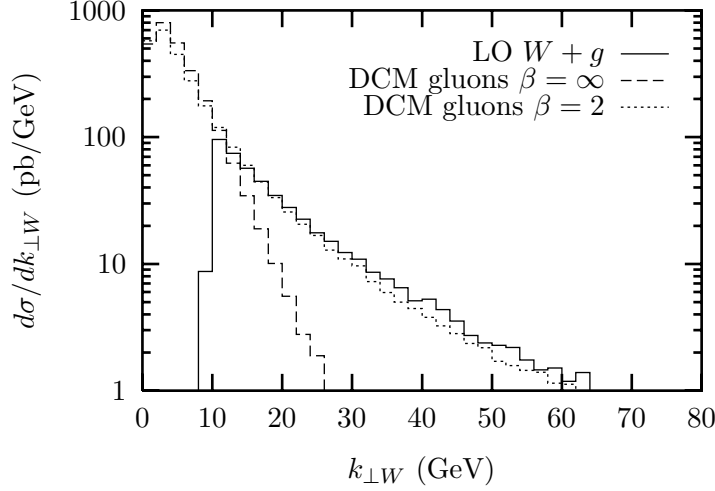


Figure 5: *The transverse momentum spectrum of the W at the Tevatron. The full line is the prediction of the $\mathcal{O}(\alpha_S)$ $W + g$ matrix element as implemented in PYTHIA using CTEQ2L parton density functions. The matrix element calculation was cut off at $k_{\perp W} = 10$ GeV to avoid divergences. The dashed and dotted lines are the predictions of the gluon emission in the DCM with $\beta = \infty$ and $\beta = 2$, respectively.*

clear, however, that such a power suppression would greatly influence the high- k_{\perp} spectrum of the W .

First, however, the way of obtaining a transverse momentum of the W in the gluon emissions must be formalized. It is clear that, in the first emission, the gluon corresponds unambiguously to initial state radiation, and hence the k_{\perp} of the gluon must be balanced by the k_{\perp} of the W . In further emissions this is not the case, as the dipole radiation is a coherent sum of the emission from the incoming partons and the outgoing, previously radiated, gluon. It is therefore argued that only gluon radiation that takes place close to the W in phase space should be able to influence the k_{\perp} of the W ; only gluons emitted in the shaded region of fig. 4, corresponding to $P_{g+} < P_{W+}$ and $P_{g-} < P_{W-}$, will have their transverse recoil absorbed by the W . Outside this region the transverse recoil will be treated as in the DIS case above.

Figure 5 shows the $\mathcal{O}(\alpha_S)$ $W + g$ matrix element prediction (as implemented in PYTHIA) of the k_{\perp} spectrum of the W at the Tevatron, compared to the modified DCM described above. With a sharp cutoff in the phase space, it is clear that the DCM cannot describe the high- k_{\perp} tail of the spectrum. Instead, a smooth suppression can be introduced by changing eq. (1), allowing a larger fraction a' of the remnant to take part in the emission with the probability

$$P(a') \propto \frac{\beta(\frac{a'}{a})^{\beta}}{a'(1 + (\frac{a'}{a})^{\beta})^2}, \quad (11)$$

corresponding to a smoothening of the theta function suppression in fig. 4, giving a power-suppressed tail. As seen in fig. 5, using $\beta = 2$ describes well the high- k_{\perp} spectrum obtained

from the leading-order calculation using the CTEQ2L¹ [24] structure function parametrization. In the following, this value of β will be used, unless stated otherwise.

This concludes the description of the W + gluon jet in the DCM. However, at small x , the gluon density in the proton becomes very large, and the Compton diagrams in fig. 2b are dominating.

3 The Compton Diagrams

The matrix element for the Compton diagrams looks like [23]

$$M^{gq \rightarrow Wq} \propto -\frac{\hat{s}^2 + \hat{t}^2 + 2m_W^2 \hat{u}}{\hat{s}\hat{t}}. \quad (12)$$

The s -channel diagram is, of course heavily suppressed for small k_\perp , and looking only at the t -channel diagram, convoluting with parton densities and factoring out the zeroth order W production cross section, as in the gluon emission case above, the normal leading log initial-state parton shower cross section for the splitting of an incoming gluon into a $q\bar{q}$ pair [25] is obtained:

$$d\sigma_q = \frac{\alpha_S}{4\pi} (z^2 + (1-z)^2) \frac{f_g(x/z)}{f_q(x)} \frac{dz}{z} \frac{dQ^2}{Q^2}, \quad (13)$$

where $Q^2 = -\hat{t}$ and $z = m_W^2/\hat{s}$.

In the DCM, however, there is no initial state gluon splitting into $q\bar{q}$, and, just as in the case of final-state $g \rightarrow q\bar{q}$ splitting [26], this process has to be added by hand to the DCM.

The simplest way is to introduce the initial-state $g \rightarrow q\bar{q}$ splitting in the same way as in [26], as a process competing with the DCM gluon emission described above. The competition is as usual governed by the Sudakov form factor using ordering in k_\perp^2 . Rewriting eq. (13) in terms of the transverse momentum k_\perp^2 and rapidity y_q of the outgoing quark, the probability of the *first* emission to be an initial-state $g \rightarrow q\bar{q}$ splitting at a certain k_\perp^2 and y_q is given by

$$\begin{aligned} \frac{dP_q(k_\perp^2, y_q)}{dk_\perp^2 dy_q} &= \frac{d\sigma_q(k_\perp^2, y_q)}{dk_\perp^2 dy_q} \times \\ &\exp - \int_{k_\perp^2}^{k_{\perp\max}^2} dk_\perp'^2 \int dy_q' \left(\frac{d\sigma_q(k_\perp'^2, y_q')}{dk_\perp'^2 dy_q'} + \frac{d\sigma_g(k_\perp'^2, y_q')}{dk_\perp'^2 dy_q'} \right), \end{aligned} \quad (14)$$

where the second factor is the Sudakov form factor, corresponding to the probability *not* to have any emission of gluons *or* gluon splittings above the scale k_\perp^2 .

¹The CTEQ2L structure function parametrization is used in all analyses in this paper where applicable. None of the conclusions in this paper were found to be sensitive to this choice.

Technically, the extra process is implemented as follows. If the quark going into the hard interaction on one side is a sea-quark, the remnant on that side is allowed to “radiate” the corresponding antiquark according to eq. (13). After such an emission, the remnant is split in two parts according to the prescription described in ref. [21], one of which forms a dipole with the “emitted” antiquark while the other retains the dipole colour connection of the original remnant.

If the first emission is a $g \rightarrow q\bar{q}$ splitting, the full $\mathcal{O}(\alpha_S)$ matrix element is used, and the rapidity of the W is assumed to be the same before and after the emission, as in the gluon emission case. A splitting later on in the cascade, the kinematic is fixed by requiring the non-radiating remnant to be unchanged. In all cases, the transverse momentum of the struck system will of course balance the k_\perp of the emitted antiquark. Note that only one initial state $g \rightarrow q\bar{q}$ splitting is allowed per remnant. This is a good approximation, since a second such splitting is heavily suppressed by the parton density functions.

This procedure can be used not only in the case of W production, but for all processes with a hadron remnant present. In particular it can be (and is²) applied in the DIS case.

In fig. 6a, the W k_\perp spectrum at the Tevatron is shown, using the full $\mathcal{O}(\alpha_S)$ matrix element (as implemented in PYTHIA) and using the modified DCM with the initial state $g \rightarrow q\bar{q}$ splitting as implemented in ARIADNE³. Clearly the DCM does a good job of reproducing the high- k_\perp tail of the distribution. In fig. 6b the DCM is compared with the two parton shower approaches of PYTHIA, one using only parton showers and one using first-order matrix elements with parton shower added. Since the DCM is a leading-log cascade, except that the first emission is uses the full matrix element, it smoothly interpolates between the pure parton shower description, which should be a good approximation for small k_\perp , and the matrix element description, which is good for high k_\perp , but has to be cut off at small k_\perp to avoid divergences.

4 Results and Predictions

In ref. [18], it was found that, when looking at the rapidity of the balancing jet in high- k_\perp W events at the Tevatron, no correlation with the W rapidity was found, while a leading order and a next to leading order calculation predicted a strong correlation. It was also found that a preliminary implementation of the DCM model described here reproduced data fairly well and only gave a very weak correlation⁴.

²This is the default in ARIADNE version 4.06 and later.

³All results labelled ARIADNE or DCM are actually generated using the zeroth-order W production in PYTHIA, with the CDM added and, where indicated, using the string fragmentation implemented in JETSET [12].

⁴The results presented here differ from the ones in ref. [18] due to a bug introduced in the initial-state $g \rightarrow q\bar{q}$ splitting in the preliminary version of ARIADNE used in that paper.

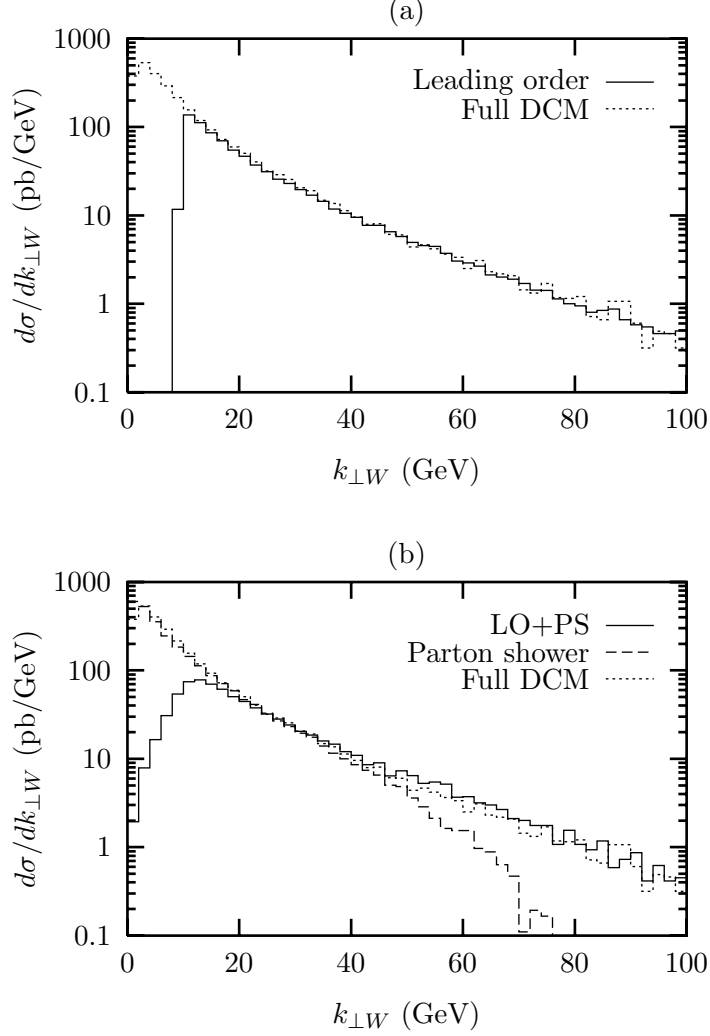


Figure 6: *The transverse momentum spectrum of the W at the Tevatron. In (a) the full line is the prediction of the full $\mathcal{O}(\alpha_S)$ W +jet matrix element as implemented in PYTHIA. The dotted line is the prediction of the full DCM with $\beta = 2$ and initial-state $g \rightarrow q\bar{q}$ splitting. In (b) the full line is as in (a) but with the parton shower of PYTHIA added after the first emission, the dashed line is PYTHIA using only parton showers and the dotted line is the same as in (a).*

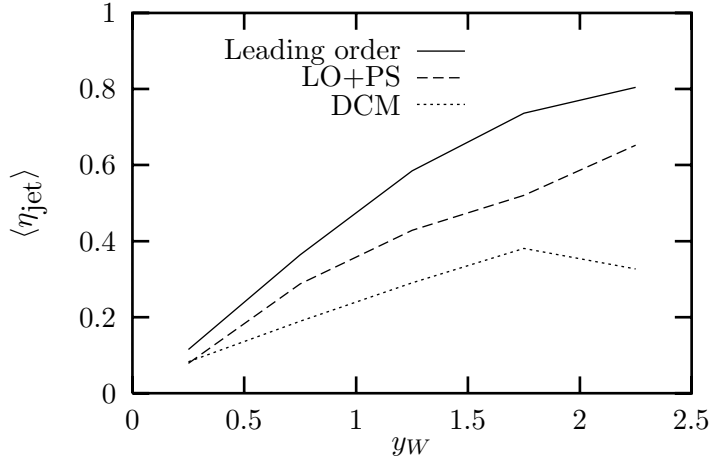


Figure 7: *The average jet pseudo-rapidity η vs. the rapidity of the W y_W at the Tevatron. The jets are reconstructed with a cone algorithm using a radius of 0.7, and in each event a jet with $E_\perp > 20$ GeV, and $|\eta| < 3$ on the opposite side in azimuth w.r.t. the W , is selected. In case of several such jets, the one with E_\perp closest to the k_\perp of the W is chosen. The full line is the leading order calculation as implemented in PYTHIA, the dashed line is the same, but with parton showers and fragmentation added, and the dotted line is the full DCM also with fragmentation added. (The “kinkiness” of the lines are due to limited statistics in the simulations.)*

Figure 7 is an attempt to reconstruct the measurement in ref. [18]⁵ on the generator level. As expected from eqs. (6) and (12), which are both symmetric around the W rapidity, the leading-order calculation gives a more or less linear correlation between the mean jet pseudo-rapidity and the rapidity of the W , although $\langle \eta_{\text{jet}} \rangle \neq y_q$ due to the smearing of the structure function convolution and the limited kinematical acceptance for jets.

When parton showers and fragmentation are added to the leading-order calculation, the smearing is increased. Also, since the phase space available for emissions is larger on the side where the x of the incoming parton is smaller, the jets for large y_W are “dragged” somewhat towards the centre, destroying the correlation. In the DCM, this dragging is more pronounced due to the ordering in the cascade as follows.

In the parton shower in PYTHIA, each step in the backward evolution of the initial-state shower is ordered in both x and virtuality Q^2 ; thus even if the phase space is larger on the small- x side of the W , the shower quickly runs out of phase space due to the ordering in Q^2 (resulting also in an ordering in k_\perp^2) as in fig. 8a. The DCM, although ordered in k_\perp^2 , is not ordered in x , or, if the final state partons are traced backwards in colour from the hard interaction, ordered in x but *not* in k_\perp^2 as in fig. 8b. In this respect, the DCM is similar to the BFKL evolution, and it gives a good description of the large transverse energy flows in

⁵The details in the jet reconstruction may differ from that of ref. [18]. In addition, the experimental ambiguity in the y_W determination is not taken into account here.

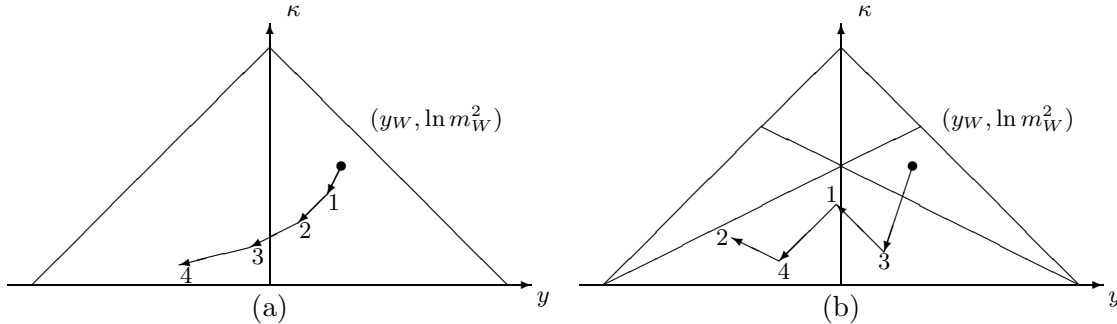


Figure 8: *Example of paths, tracing emissions backwards from the hard interaction $(y_W, \ln m_W^2)$ on the small- x side of high-rapidity W events for (a) the initial-state parton shower in PYTHIA, where the emissions are ordered both in x and k_\perp^2 , and (b) the DCM, where the emissions, although the cascade is ordered in k_\perp^2 , when traced backwards from the hard interaction in this way, are ordered in x but not in k_\perp^2 .*

small- x events at HERA, which has been suggested as a signal for the BFKL evolution [11]. Because of this, the DCM can better use the increased phase space on the small- x side of the W and the “dragging” effect is larger than for conventional parton showers in fig. 7, and the result closer to, if not consistent with, the measurement in ref. [18].

The increase in transverse energy flow at small x found at HERA should also be visible at the Tevatron in high-rapidity W events. In fig. 9 the predictions for the E_\perp flow from the parton shower model of PYTHIA⁶ and the DCM of ARIADNE are shown for inclusive W events at the Tevatron for two W rapidity intervals. The two models are fairly similar at central W rapidities, while for high y_W the DCM gives more transverse energy, despite the fact that the hard interaction scale ($m_W^2 \approx 6400 \text{ GeV}^2$) is much larger here than at HERA ($\langle Q^2 \rangle \lesssim 100 \text{ GeV}^2$).

In pp collisions we also have to worry about underlying events. In fig. 7, this does not give large effects since a large- E_\perp jet is required, but for fig. 9 the underlying event would give an extra contribution to the E_\perp flow. This extra contribution should however be evenly spread out in η and independent of y_W , and the differences between the parton shower and DCM approaches should survive. To take this contribution into account, the multiple interaction model implemented in PYTHIA [27] has been used. Note, however, that in the case of the DCM, only the qualitative features of the contribution are completely relevant, as the parameters of the multiple interaction model probably need to be retuned to fit the DCM.

The differences between the parton shower and the DCM approaches are most significant when the E_\perp flow is measured as a function of y_W as in fig. 10, where the E_\perp flow, two

⁶Since no high- k_\perp jets are required and the bulk of the events are at low $k_{\perp W}$, the matrix element plus parton shower approach in fig. 7 is not adequate here.

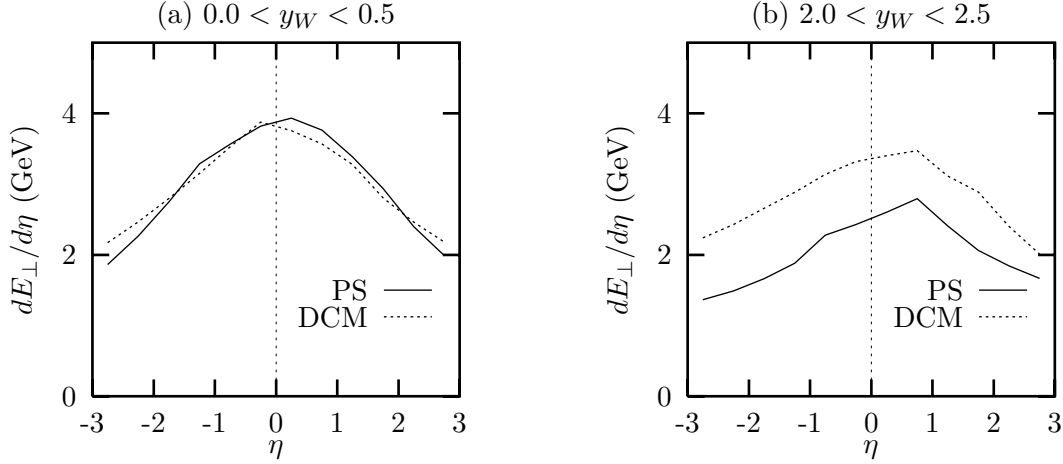


Figure 9: The transverse energy flow in inclusive W events at the Tevatron for (a) $0.0 < y_W < 0.5$ and (b) $2.0 < y_W < 2.5$. The full and dotted lines are the predictions of the DCM in ARIADNE and of the parton shower in PYTHIA, respectively.

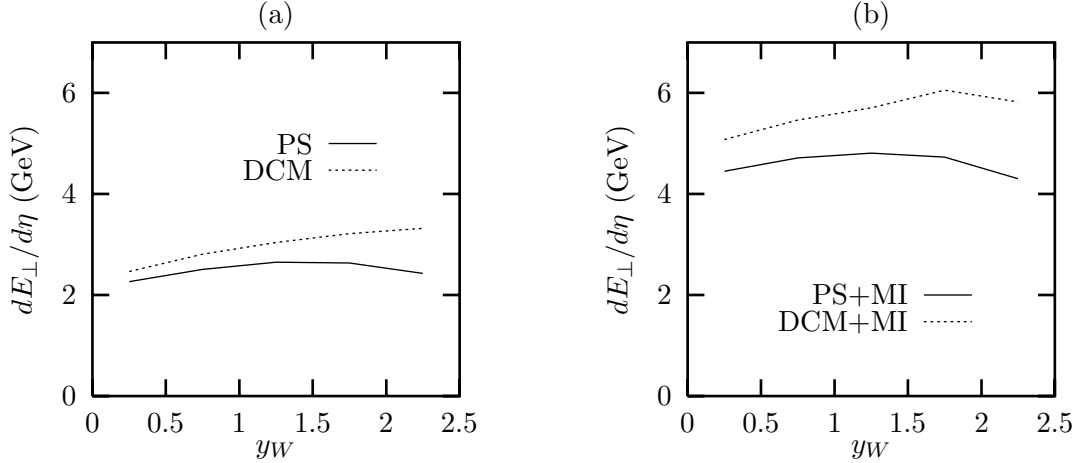


Figure 10: The transverse energy flow two units of rapidity “behind” the W for inclusive W events, at the Tevatron, i.e. for the interval $1.0 < y_W < 1.5$ the E_\perp flow in the pseudo-rapidity interval $-1.5 < \eta < -1.0$. The full line is the PYTHIA parton shower and the dotted line is the DCM without (a) and with (b) multiple interactions.

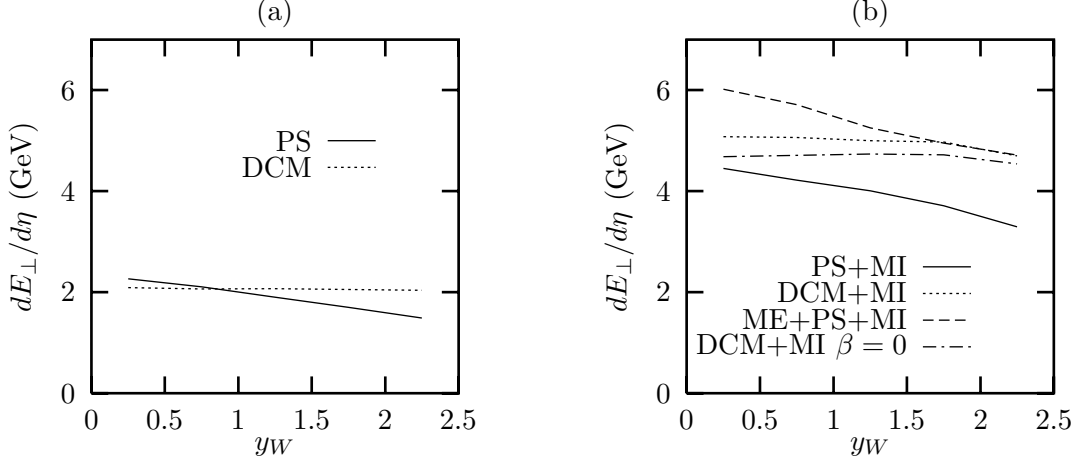


Figure 11: The transverse energy flow in the interval $-2.5 < \eta < -2.0$ for W events at the Tevatron as a function of y_W . The full line is the PYTHIA parton shower and the dotted line is the DCM without (a) and with (b) multiple interactions. In (b) the dashed line is PYTHIA using $\mathcal{O}(\alpha_S)$ matrix elements with addition of parton showers and multiple interactions, and the dash-dotted line is the DCM with $\beta = \infty$.

units of rapidity away from the W , is shown for both models, with and without the multiple interaction model for the underlying event implemented in PYTHIA [27]. It is clear that the underlying event introduces an extra E_{\perp} for both models, but that the dependence of the E_{\perp} flow on y_W is still different for the two models. As expected the E_{\perp} flow is more or less constant for the parton shower approach, but increases slightly for the DCM due to the increase in phase space at large y_W .

Similarly, looking at the E_{\perp} flow in a fixed rapidity interval for varying y_W , the DCM predicts a fairly constant value, while in the parton shower approach, the flow decreases with increasing y_W as in fig. 11. To check that the differences are not due to the fact that the DCM has the correct $\mathcal{O}(\alpha_S)$ matrix element in the first emission, fig. 11b also contains a line with the matrix element plus parton shower option in PYTHIA. It is clear that, although the E_{\perp} flow is higher since only events with $k_{\perp W} > 10$ GeV are included, it has the same y_W dependence as the plain parton shower approach.

Also in fig. 11, the changing of the β parameter in the DCM is shown to have some effect on the E_{\perp} flow; however, the dependence on y_W is still the same.

5 Conclusions

The model presented in this paper is not perfect. The treatment of initial-state $g \rightarrow q\bar{q}$ splitting is a bit foreign to the original Colour Dipole Model, and so is the transfer of

transverse recoil to the W for gluon emissions. But as a leading log approximation it should be just as good as the conventional parton shower approach, and it has the advantage of correctly describing also high- k_\perp W production. In addition it gives the opportunity of studying effects of unordered parton evolution on the hadronic final state, and, although there are some uncertainties in the overall E_\perp level due to multiple interactions and the β parameter in the DCM, it would be very interesting to compare the predictions for the y_W dependence of the E_\perp flow presented in this paper with data from the Tevatron.

Although only W production at the Tevatron has been discussed in this paper, the model can of course be applied to any Drell–Yan-like process in any hadron–hadron collision. And, as pointed out above, the initial-state $g \rightarrow q\bar{q}$ splitting can be used also in deep inelastic lepton–hadron scattering.

The model presented here is also the “last piece” to complete the DCM description of QCD cascades for all standard processes in e^+e^- , ep and pp collisions. This is reflected in the fact that ARIADNE now is fully interfaced to all hard sub-processes in PYTHIA. However, some care must be taken when using the multiple interaction model of PYTHIA together with the DCM, as mentioned above.

Acknowledgements

I would like to thank Bo Andersson and Gösta Gustafson for valuable discussions.

References

- [1] H1 COLL., I. ABT ET AL., *Nucl. Phys. B* **407** (1993) 515.
- [2] ZEUS COLL., M. DERRICK ET AL., *Phys. Lett. B* **316** (1993) 412.
- [3] V.S. FADIN, E.A. KURAEV, L.N. LIPATOV, *Sov. Phys. JETP* **45** (1977) 199.
- [4] YA.YA. BALITSKY, L.N. LIPATOV, *Sov. J. Nucl. Phys.* **28** (1978) 822.
- [5] R.D. BALL, S. FORTE, *Phys. Lett. B* **335** (1994) 77.
- [6] R.D. BALL, S. FORTE, *Phys. Lett. B* **336** (1994) 77.
- [7] V.N. GRIBOV, L.N. LIPATOV, *Sov. J. Phys.* **15** (1972) 438 and 675.
- [8] L.N. LIPATOV, *Sov. J. Phys.* **20** (1975) 94.
- [9] G. ALTARELLI, G. PARISI, *Nucl. Phys. B* **126** (1977) 298.
- [10] YU.L. DOKSHITSER, *Sov. Phys. JETP* **46** (1977) 641.

- [11] J. KWIECIŃSKI ET AL., *Phys. Rev. D* **50** (1994) 217.
- [12] T. SJÖSTRAND, *Comput. Phys. Commun.* **82** (1994) 74.
- [13] T. SJÖSTRAND, PYTHIA 5.7 and JETSET 7.4 physics and manual, CERN-TH.7112/93, Dec. 1993, (revised Aug. 1994).
- [14] G. INGELMAN, LEPTO version 6.1, in *Physics at HERA*, edited by W. BUCHMÜLLER, G. INGELMAN, volume 3, p. 1366, DESY, 1991.
- [15] L. LÖNNBLAD, ARIADNE version 4.07 program and manual, *Comput. Phys. Commun.* **71** (1992) 15.
- [16] H1 COLL., I. ABT ET AL., *Z. Phys. C* **63** (1994) 377.
- [17] H1 COLL., I. ABT ET AL., Transverse Energy and Forward Jet Production in the Low x Regime at HERA, DESY-94-133, June 1995.
- [18] D0 COLL., G.E. FORDEN ET AL., Probing color coherency using high p(t) W events at the Tevatron, preprint AZPH-EXP-94-01, August 1994.
- [19] G. GUSTAFSON, *Phys. Lett. B* **175** (1986) 453.
- [20] G. GUSTAFSON, U. PETTERSSON, *Nucl. Phys. B* **306** (1988) 746.
- [21] B. ANDERSSON ET AL., *Z. Phys. C* **43** (1989) 625.
- [22] L. LÖNNBLAD, *Z. Phys. C* **65** (1995) 285.
- [23] F. HALZEN, M. SCOTT, *Phys. Rev. D* **18** (1978) 3378.
- [24] CTEQ COLL., J. BOTTS ET AL., *Phys. Lett. B* **304** (1993) 159.
- [25] M. BENGTSSON, T. SJÖSTRAND, *Z. Phys. C* **37** (1988) 465.
- [26] B. ANDERSSON, G. GUSTAFSON, L. LÖNNBLAD, *Nucl. Phys. B* **339** (1990) 393.
- [27] T. SJÖSTRAND, M. VAN ZIJL, *Phys. Rev. D* **36** (1987) 2019.